



# Potential for western US seasonal snowpack prediction

Sarah B. Kapnick<sup>a,1</sup>, Xiaosong Yang<sup>a,b</sup>, Gabriel A. Vecchi<sup>c,d</sup>, Thomas L. Delworth<sup>a</sup>, Rich Gudgel<sup>a</sup>, Sergey Malyshev<sup>a,e</sup>, P. C. D. Milly<sup>f</sup>, Elena Shevliakova<sup>a,d</sup>, Seth Underwood<sup>a</sup>, and Steven A. Margulis<sup>g</sup>

<sup>a</sup>Geophysical Fluid Dynamics Laboratory, National Oceanic and Atmospheric Administration, Princeton, NJ 08540; <sup>b</sup>Cooperative Programs for the Advancement of Earth System Science, University Corporation for Atmospheric Research, Boulder, CO 80307; <sup>c</sup>Geosciences, Princeton University, Princeton, NJ 08544; <sup>d</sup>Princeton Environmental Institute, Princeton University, Princeton, NJ 08544; <sup>e</sup>Ecology and Evolutionary Biology, Princeton University, Princeton, NJ 08540; <sup>f</sup>Integrated Modeling and Prediction Division, Water Mission Area, United States Geological Survey, Princeton, NJ 08540; and <sup>g</sup>Civil and Environmental Engineering, University of California, Los Angeles, CA 90095

Edited by Thomas Dunne, University of California, Santa Barbara, CA, and approved December 11, 2017 (received for review September 27, 2017)

**Western US snowpack—snow that accumulates on the ground in the mountains—plays a critical role in regional hydroclimate and water supply, with 80% of snowmelt runoff being used for agriculture. While climate projections provide estimates of snowpack loss by the end of the century and weather forecasts provide predictions of weather conditions out to 2 weeks, less progress has been made for snow predictions at seasonal timescales (months to 2 years), crucial for regional agricultural decisions (e.g., plant choice and quantity). Seasonal predictions with climate models first took the form of El Niño predictions 3 decades ago, with hydroclimate predictions emerging more recently. While the field has been focused on single-season predictions (3 months or less), we are now poised to advance our predictions beyond this timeframe. Utilizing observations, climate indices, and a suite of global climate models, we demonstrate the feasibility of seasonal snowpack predictions and quantify the limits of predictive skill 8 months in advance. This physically based dynamic system outperforms observation-based statistical predictions made on July 1 for March snowpack everywhere except the southern Sierra Nevada, a region where prediction skill is nonexistent for every predictor presently tested. Additionally, in the absence of externally forced negative trends in snowpack, narrow maritime mountain ranges with high hydroclimate variability pose a challenge for seasonal prediction in our present system; natural snowpack variability may inherently be unpredictable at this timescale. This work highlights present prediction system successes and gives cause for optimism for developing seasonal predictions for societal needs.**

cryosphere | seasonal prediction | climate | water | snowpack

The majority of annual precipitation in the western United States (WUS) accumulates between October and April, falling as snow in the mountains (1). As a result, snow accumulation forms mountain snowpack, peaking in early spring and melting into the summer, dominating runoff and influencing lower-elevation streamflow (2). WUS mountain snowpack therefore provides a natural reservoir for winter precipitation, as it supplies snowmelt runoff when temperatures are above freezing and regional precipitation is otherwise scarce from late spring through fall (3, 4).

Springtime snowpack has been observed to have reduced in the last century (5, 6) and recently reached an unprecedented low (7), altering the timing of regional runoff, creating competing demands for water use (8), stressing ecology (8, 9), and increasing the risk of wildfire (10). Seasonal climate predictions would therefore be of great societal relevance to agriculture, water managers, and policy makers to plan for annual climate deviations.

Previous work exploring seasonal prediction in global climate models has focused on the El Niño–Southern Oscillation (ENSO) (11), total precipitation (12), and temperature (13); snowpack prediction has not been a primary focus. Knowing future precipitation or temperature alone is, unfortunately, insufficient for snowpack prediction; for example, knowing it will be a wet year does not guarantee a large spring snowpack if temperatures are above freezing. Previous work has quantified the multiseasonal (November–March) covariance of observed WUS snowpack point

measurements and climate indices for ENSO (14–17), Pacific Decadal Oscillation (PDO) (14, 18), the Pacific–North American (PNA) circulation pattern (17, 19), and the Madden–Julian Oscillation (MJO) (20). These climate indices explain limited variance and do not cohesively explain WUS snowpack (14, 16). Moreover, the links between climate indices and snowpack have been made with averaged seasonal indices, identifying the covariance of index values over several months through March with April snowpack values, rendering them inapplicable for multi-month out-of-season predictive applications (14–19). The relatively short instantaneous snowpack measurement record (<40 y) (5) also complicates our ability to predict WUS snowpack from observations alone, particularly extremes, given the sample size (21).

Advancements in understanding subseasonal to single-season (<3 mo) hydroclimate prediction and variability have been made, but should not be extrapolated to an expectation of multi-seasonal predictive skill. For example, certain phases of the MJO have been linked to atmospheric rivers and snowpack accumulation over California (20), but only in specific phases of the MJO, with atmospheric rivers climatologically only accounting for 30 to 40% of snowpack accumulation in California (22). Statistical and dynamical models also have no demonstrated prediction skill for the MJO beyond a 2- to 4-wk lead time (23, 24). Understanding the role of the MJO is important for advancing the understanding of extreme precipitation in California, even if it does

## Significance

Mountain snowpack in the western United States provides a natural reservoir for cold season precipitation; variations in snowpack influence warm season water supply, wildfire risk, ecology, and industries like agriculture dependent on snow and downstream water availability. Efforts to understand snowpack variability have predominantly been focused on either weekly (weather) or decadal to centennial (climate variability and change) timescales. We focus on a timescale between these ranges by demonstrating that a global climate model suite can provide snowpack predictions 8 months in advance. The predictions from climate models outperform statistical methods from observations alone. Our results show that seasonal hydroclimate predictions are possible and highlight areas for future prediction system improvements.

Author contributions: S.B.K. designed research; S.B.K. performed research; S.B.K., X.Y., and S.A.M. contributed new reagents/analytic tools; S.B.K., X.Y., and S.A.M. analyzed data; and S.B.K., X.Y., G.A.V., T.L.D., R.G., S.M., P.C.D.M., E.S., S.U., and S.A.M. wrote the paper.

The authors declare no conflict of interest.

This article is a PNAS Direct Submission.

Published under the PNAS license.

Data deposition: The data reported in this paper have been deposited in the Geophysical Fluid Dynamics Laboratory Data Portal (available at [data1.gfdl.noaa.gov](http://data1.gfdl.noaa.gov)).

<sup>1</sup>To whom correspondence should be addressed. Email: [sarah.kapnick@noaa.gov](mailto:sarah.kapnick@noaa.gov).

This article contains supporting information online at [www.pnas.org/lookup/suppl/doi:10.1073/pnas.1716760115/-DCSupplemental](http://www.pnas.org/lookup/suppl/doi:10.1073/pnas.1716760115/-DCSupplemental).

not provide seasonal prediction skill on a consistent basis (e.g., for other MJO phases), for the WUS as a whole, or on longer timescales (23, 24). More generally, multiseasonal prediction skill is a different scientific question than single-season prediction. As the ocean and climate states evolve, predictions become less dependent on knowing the atmospheric initial climate state for prediction (why statistics are successful at shorter timescales) and transition to being based on oceanic and radiative boundary conditions and the ability to predict the evolution of climate (25).

In this study, we highlight seasonal 8-mo-lead predictions initialized on July 1 for March WUS snowpack from three atmosphere–ocean general circulation models (AOGCM) developed at the Geophysical Fluid Dynamics Laboratory (GFDL). The three AOGCMs share a similar ocean, but differ in their horizontal atmospheric/land resolutions (200, 50, and 25 km; refs. 26–28), resulting in increasing orographic fidelity (*SI Appendix, Fig. S1*). AOGCM multimember ensemble hindcasts (10 for 200 km, and 12 for 50 and 25 km) following refs. 13 and 28 were initialized by data assimilation of the ocean (29) with land states from climatology (see *Materials and Methods*) on July 1 of every year (1980–2015). Starting from these July 1 initial conditions, the dynamical model then predicted the evolution of the climate system over the following year, allowing us to assess predicted snowpack values for the following March (1981–2016). Results utilize ensemble mean predictions except where noted. Statistical models are also tested by using observed climate indices available on July 1 to contrast our dynamical AOGCM predictions. The dynamical physical models and statistical models are verified against snow water equivalent (SWE) observations and reanalysis.

### Prediction Skill for March Snowpack Using Initial Conditions from July of the Prior Year

Fig. 1 shows the ability of the AOGCMs to reproduce average March snowpack. This multiresolution modeling framework clearly illustrates the role of horizontal resolution for improving simulation of snowpack climatology (Fig. 1). At 200 km, mountains are smooth and low (*SI Appendix, Fig. S1*), resulting in minimal SWE confined to the interior continent (30). At 50 and 25 km, the models reproduce finer-scale maritime mountain features with SWE values approaching observations; snowpack bias across the WUS decreases with resolution (*SI Appendix, Fig. S2*). Biases in the absolute value of snowpack may be limited by resolution restricting topographic height and therefore snow accumulation (30). As a result, snowpack anomalies normalized

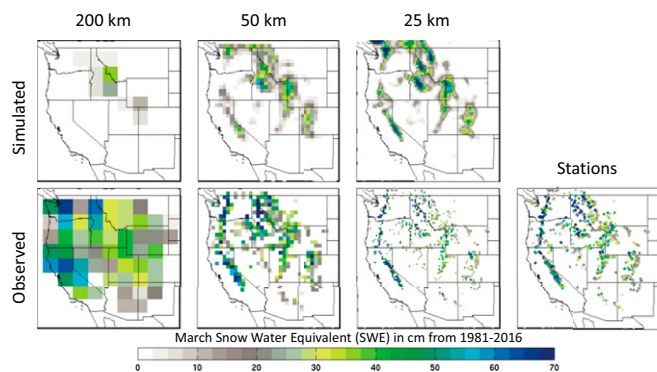


**Fig. 1.** Mean March snowpack climatology for 1981–2016 at each model resolution (noted in the column headers). Observations (*Bottom*) are taken from snowpack point measurements (*Right*) and are regridded to native model grids. Simulated climatology of ensemble mean spring prediction values from previous July (8 mo in advance; *Top*) from three GFDL AOGCMs (described in *Materials and Methods*). Spatial resolution is coarsest in *Left* and finest in *Right* (200 km is the lowest resolution).

by regional means provide a relative comparison across resolutions; this metric leads to the WUS normalized anomaly bias approaching 0 (*SI Appendix, Fig. S3*).

Fig. 2 provides a case study of the recent 2012–2015 multiyear southern WUS snowpack drought. All of the AOGCMs roughly reproduce the observed pattern of anomalously low (high) snowpack in the southwest (northeast). In this case study using ensemble mean predictions, the 50-km model appears to perform the best, while the 25-km model incorrectly predicts highs in the southern WUS.

The ability of the modeling suite to reproduce average 1981–2016 March snowpack and roughly predict the recent snowpack drought motivates us to further explore prediction skill across the entire record and all models (both individually and as a suite). Fig. 3 provides regional seasonal prediction metrics; for each mountain region, the regional averaged AOGCM March snowpack prediction made on July 1 the previous year is correlated with the observed March snowpack value. The higher-resolution AOGCMs consistently (both individually and as multimodel means) produce positive statistically significant correlations across all regions except in the southern Sierra Nevada and in Washington State.

### Role of Initial Climate State

Seasonal snowpack prediction skill exists in our AOGCM suite based on the initialization of the ocean (on July 1) and the dynamic development of the coupled system (as the AOGCMs simulate climate through March 31). We therefore contrast our dynamical AOGCM predictions with static observed statistical predictions (based on the initial state known at July 1 alone) by correlating available observed climate indices (ENSO, PNA, and PDO) at July 1 with the following March snowpack. This also tests whether indices with known intraseasonal snowpack covariance could be used for out-of-season predictions. The PDO does not have prediction skill in any region, despite demonstrated correlations at shorter time scales (14, 18). ENSO only has statistically significant prediction skill in the Northern Rockies, but with a lower absolute value than the AOGCMs. The PNA pattern is the only climate index with consistent predictive skill (Fig. 3), yet it is also an atmospheric index, with expectations for shorter timescales of persistence and predictability than ocean-based indices like ENSO (31). Its predictive skill may reflect seasonal consistency in storm track position through February (32), lending itself to longer-range seasonal snowpack prediction skill.

The AOGCMs consistently outperform the static statistical predictions, with the multimodel mean of the higher-resolution models (mean of the 50- and 25-km model ensemble mean predictions; Fig. 3, black triangles) generally outperforming individual model predictions. This suggests that two factors may enhance skill: (i) the doubling of ensemble members to sample a greater set of possible solutions or (ii) differences in model biases found individually in the 50- and 25-km models that are reduced when combined. The one exception is the southern Sierra Nevada, where no predictor is statistically significant.

### Challenges of the Sierra Nevada

The southern Sierra Nevada is an elongated mountain range (Fig. 1 and *SI Appendix, Fig. S1*) with the highest peak in the contiguous United States, Mount Whitney (4.4 km); this region may require even higher resolutions than our system to achieve mountain heights (presently our tallest is 3.4 km in the 25 km model) for sufficient orographic precipitation and cold temperatures for snowpack dynamics. This region is characterized by narrow and infrequent storms—less than 10 per year, with some years receiving the majority of snowpack from a single storm (33, 34)—and some of the most variable snowpack (*SI Appendix, Figs. S4 and S5*). The higher-resolution models capture the spatial patterns of interannual variability, but with lower magnitudes than observed. This high natural variability and bias in the models

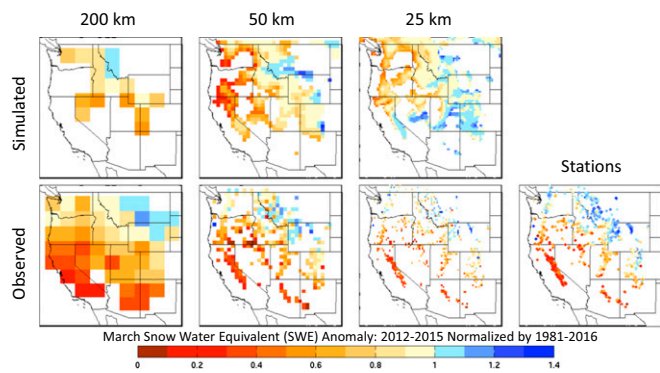


**Fig. 2.** As in Fig. 1, observed (*Bottom*) and ensemble mean simulated AOGCM March predictions from previous July (*Top*) of snowpack anomalies in 2012–2015 relative to 1981–2016 mean. Note that, for simulated plots, points have been masked for only those with climatological (1981–2016) simulated SWE greater or equal to 1 cm.

may make it inherently more difficult to predict Sierra Nevada snowpack, particularly if the few storms that happen in a year are shifted outside the defined region.

We attempt to reduce the impact of storm location error by aggregating the Sierra Nevada, maritime mountains (Sierra Nevada, Oregon Cascades, Washington State), and the entire WUS region (Fig. 3*B*). This allows us to test larger-scale prediction skill and reduces errors caused by spatial differences in storms shifted across the region as long as they stay within the new aggregated ranges. Aggregation leads to dynamical predictions

outperforming statistical predictions everywhere. With aggregation, skill emerges across the combined Sierra Nevada and maritime mountains.

Given the observed 1981–2016 negative trend in southern WUS snowpack (*SI Appendix, Fig. S6*), we quantify whether these trends affect the predictability of snowpack. Negative statistically significant snowpack trends have been well documented since the 1950s and tied to snowmelt occurring earlier in the season (2, 5) and precipitation falling as rain instead of snow (35). These observations reflect a regional trend in warming bringing temperatures above freezing more often and reducing the snow season length. We repeat our regional analysis for detrended time series, finding that high correlation values remain similar to the original analysis (Fig. 3 and *SI Appendix, Fig. S7*). However, the AOGCM snowpack predictions lose statistical significance over the Sierra Nevada, resulting in a loss of prediction skill in the aggregated maritime mountains despite skill in Oregon and Washington. Therefore, the predictive skill in the original analysis found in Fig. 3 for the Sierra Nevada and maritime mountains came from the models’ ability to reproduce the trend of Sierra Nevada snowpack loss. This suggests that the AOGCM system cannot capture the internally forced natural variability of Sierra Nevada snowpack. We cannot conclude definitively whether this is due to a lack of predictability in the system or a model deficiency in capturing subgrid-scale orographic precipitation dynamics in a region where snowfall is highly sensitive to storm direction and vertical temperature profiles (i.e., determining transitions between rain and snow) and trends can vary in elevation (5, 6, 33, 35). For additional verification, analysis was also performed with a higher-resolution snowpack reanalysis product, starting in 1985 (ref. 36 and *SI*

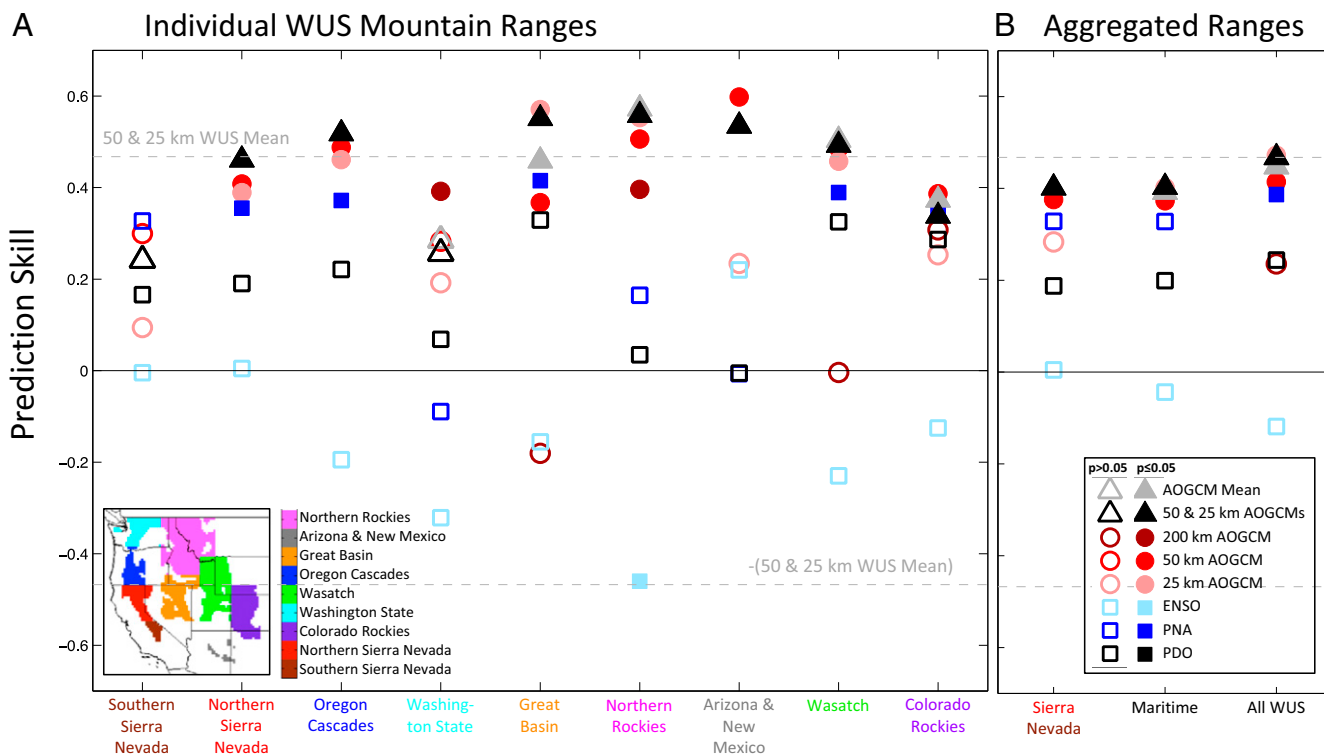


**Fig. 3.** Mountain range snowpack prediction skill measured by correlations (Spearman) between observed March snowpack and predictors available July 1 from AOGCM models (triangles, circles) or climate indices (squares) where higher absolute values represent greater skill, shown for (A) various mountain ranges and (B) ranges aggregated in increasing scale. Dashed lines provided for the value of the higher-resolution multimodel (50 km and 25 km) prediction for snowpack over the entire mountainous WUS (0.48) and the negative value (–0.48) to provide a reference for correlations with climate indices. *Inset* provided for ranges in highest-resolution model; the 200-km model has no ranges for northern and southern Sierra Nevada, Oregon Cascades, or Arizona and New Mexico (*SI Appendix, Fig. S1*).

Appendix, Fig. S8). Raw and detrended correlations with the Sierra Nevada reanalysis also yield similar prediction skill for the AOGCM system and climate indices, but with Northern California maintaining some skill in the detrended series (*SI Appendix, Fig. S9*). This product is highly correlated with our station estimates ( $r \geq 0.95$ ; *SI Appendix, Fig. S8*) and verifies that the southern Sierra Nevada is not predictable in our present system. This shows that there is regional snowpack coherence, and the station observation network is suited for integrated snowpack variability estimation.

Presently, we must conclude that Sierra Nevada snowpack is not predictable at 8-mo lead times in our prediction system without greenhouse gas forcing. AOGCM seasonal prediction skill of other phenomena—extratropical storm tracks (32), regional surface air temperature in winter and summer (25), and global surface temperature (37)—has also been linked to climate models' ability to reproduce the greenhouse gas-forced warming trends. Generally, these studies show that the otherwise unpredictable interannual variability of a specific regional climate system can become predictable in a warming climate. For Sierra Nevada snowpack, with only a few days of precipitation a year (33, 34) and a highly variable snowpack (*SI Appendix, Figs. S4 and S5*), this is due to prediction skill stemming from seasonal warming trends, leading to more precipitation falling as rain versus snow and enhanced snowmelt. Predicting the interannual variability and extreme years (either low or high snow) is precisely what decision makers need to prepare for atypical years. More work is needed with dynamical AOGCMs and observing systems customized for the Sierra Nevada and more broadly to California to (i) enhance regional prediction skill (demonstrated in *SI Appendix, Fig. S9*) or (ii) elucidate if longer lead times are unattainable due to the nature of Sierra Nevada snowpack. Other hydroclimate variables may also have better longer-lead prediction skill and should be explored.

### Enhancing Seasonal Snowpack Predictions

To identify potential model improvements vis-à-vis mechanisms affecting snowpack, we also quantify prediction skill in the higher-resolution models for precipitation, temperature, and storm tracks (32) (Fig. 4). Precipitation predictive skill is most evident in the medium-resolution model, with storm tracks tending to follow precipitation skill. The highest-resolution model has the greatest skill in temperature in the northeastern WUS, corresponding to the region where it has greatest skill in snowpack prediction (Fig. 3). Interestingly in the reproduction of climatology, the AOGCMs are stormier, wetter, and cooler than observations, with slightly larger biases in the 25-km model (*SI Appendix, Fig. S11*). This may reflect elevation differences between the 25-km model and observations, as no temperature lapse rate adjustments were made to model data during the area-averaging regriding process from 25 km to a uniform 50-km grid in Fig. 4 and *SI Appendix, Fig. S11*. While climatological spatial bias patterns are similar in both models (*SI Appendix, Fig. S11*), the spatial pattern and magnitude of prediction skill in interannual variability is quite different (Fig. 4).

These analyses highlight the difficulty of snowpack prediction: Individual models may simultaneously differ in predictive strength and spatial coverage of each individual variable affecting snowpack, without a clear advantage. Additionally, a model's ability to reproduce climatology does not necessarily translate to seasonal prediction skill. In the 20th century, the WUS mountains generally stayed below freezing through February, leading to March snowpack being heavily dominated by precipitation variability (5, 6). This favors a system optimized for precipitation skill. Where temperatures have a greater tendency to be at or above freezing, temperature skill becomes more important, due to surface melt and increased likelihood for rainfall. Temperature has likely become more important during the study record

as temperatures have increased and been anomalously warm during the multiyear California drought (39).

The southern Sierra Nevada currently eludes snowpack prediction. The outstanding question is whether this is due to inherent lack of predictability in the climate system or to errors in our AOGCM prediction system (e.g., insufficient resolution for steep mountains, microphysics, or inadequate initialization of the climate system). To quantify how ensemble members cluster around a solution (agnostic toward its accuracy), we calculate a coherence index, omega (40), relating the variance in the ensemble mean versus the full set of ensembles (*SI Appendix, Fig. S10*). Across all AOGCMs, the coherence index is greatest in the northern WUS. The southern Sierra Nevada, in particular, has little coherence, with a minimum in the 25-km model. We also quantify the ability of individual ensemble members to predict the ensemble mean versus how the ensemble mean predicts observations from Fig. 3. This test shows that the model predicts itself better than it predicts observations everywhere except the southern Sierra Nevada and Washington. Reviewing the mechanisms that lead to ensemble clustering in our AOGCM prediction system may allow us to improve the prediction of observations everywhere except in these two regions. Again, the southern Sierra Nevada is highlighted as a challenging area.

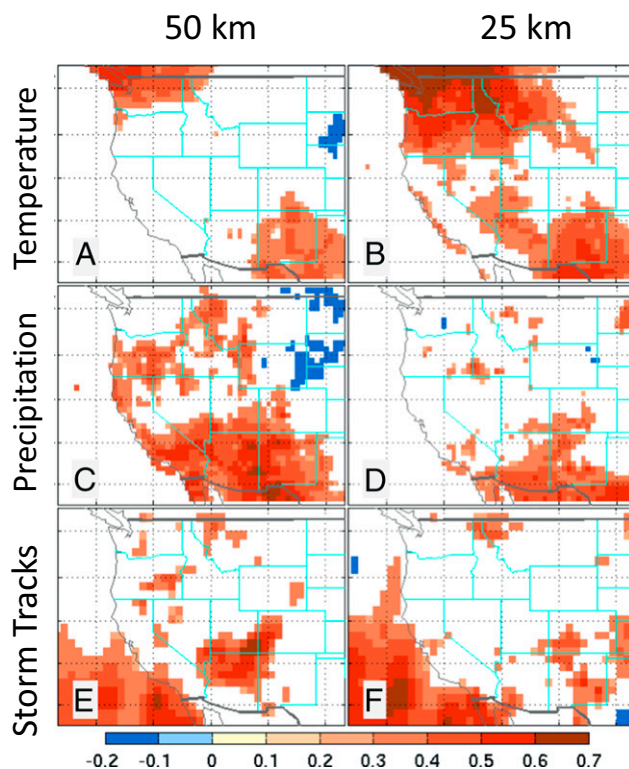


Fig. 4. Skill measured by correlation (Spearman) for temperature (A and B), precipitation (C and D), and storminess defined by 850-mb wind v-component following ref. 32 (E and F) between November 1980 and February 2015 from July 1 initialization versus 0.5° observations. Points without statistical significance ( $P > 0.1$ ) have been masked in white. Note that, unlike other prediction analyses, this figure provides predictions 4 mo in advance (from July 1 for November through February) to parse potential sources of predictability of March snowpack. Precipitation and temperature were downloaded from the University of East Anglia Climate Research Unit (<https://crudata.uea.ac.uk/cru/data/hrg/>). Wind data are from the European Reanalysis Interim product from the European Centre for Medium-Range Weather Forecasts (38).

## Discussion

Further lines of inquiry may improve seasonal snowpack prediction skill. We find that resolution enhancement from 200 km to 50 km does appear to enhance prediction skill. However, further refinement to 25 km does not markedly improve skill within this system, despite improvements in simulating mean March snowpack (Fig. 1) and tropical cyclone prediction (28). The AOGCM suite was originally developed to test the influence of resolution enhancement without dramatic changes to physics, model configuration, or initialization. At higher resolutions over complex topography, model physics (e.g., microphysics and gravity wave tuning) may dramatically affect regional precipitation and circulation, particularly in Southern California (41), requiring the development of new parameterizations. There is evidence of this in the climatology biases of variables shown in Fig. 4 being lower at 50 km than at 25 km (*SI Appendix, Fig. S11*). Higher-resolution AOGCMs may also need more ensemble members (Fig. 3, triangles versus circles) to converge on a correct solution (*SI Appendix, Fig. S10*), given the scales of atmospheric variability and increased values of localized precipitation extremes (21). Additionally, our ocean data assimilation system has not been optimized for higher-resolution atmospheres, is performed with the 200-km version of the model, and does not include atmospheric initialization with observations in the 50- and 25-km versions of the system, possibly placing the highest-resolution models at a disadvantage (29). This initialization procedure was originally developed assuming the ocean is the main driver of multiseasonal climate predictions (42), but this assumption should be tested further.

The nature of WUS snowmelt dominating spring through summer runoff extends the potential use of snowpack predictions made in July for water resources through the following summer/fall. While snowpack prediction skill is highly relevant to water resource applications and is a necessary step toward hydrologic prediction, basin-averaged streamflow should ultimately be a target for future prediction systems and will require land surface process analysis. We have purposefully dedicated this study to exploring prediction skill of spring snowpack from the previous summer, when the land surface lacks snowpack, to explore prediction skill before the first snowfall of the season. Future studies should also tie shorter lead times to snowpack prediction, but will require land surface initialization (in addition to the ocean presented here), as WUS snowpack begins to accumulate during the fall, and soil moisture becomes more important at shorter timescales (43). Additionally, testing model skill for multiday extreme weather events like atmospheric rivers will likely also be important for prediction at shorter timescales, especially in the Sierra Nevada (20, 22, 33). This work shows promise for attaining future seasonal predictions for societal needs and highlights the need for increased focus on the narrow maritime mountains as a challenging prediction problem.

## Materials and Methods

**Snowpack Observations.** Monthly first-of-the-month snowpack observations were obtained from the California Department of Water Resources Data Exchange Center ([cdcc.water.ca.gov](http://cdcc.water.ca.gov)) and the United States Department of Agriculture National Resource Conservation Service ([www.wcc.nrcs.usda.gov/snow/](http://www.wcc.nrcs.usda.gov/snow/)). Duplicate collocated measurements between the two records were removed, leaving 2,414 locations.

To create a gridded snowpack observation product for prediction system validation over 1981–2016, observed values were separated for unique months of interest, quality controlled, and gridded to native model grids. First-of-the-month observations were averaged to create monthly averages of observed snowpack (i.e., March 1 and April 1 measurements are averaged to create a mean March snowpack value). For simplicity, we have chosen to show March snowpack values across all of our analysis, which is when the snowpack historically reaches the end of its accumulation phase across the WUS (5). This also allows us to use the March 1 and April 1 station dates, which are the most robustly sampled dates spatially across the WUS, for optimal comparison with gridded model output. We next selected locations

with a minimum of 32 y of measurements (89% of years) to remove errors generated from stations dropping in and out of the record. This is a conservative assumption for assessing snowpack trends (6, 44). This leaves us with 1,136 stations in total, 136 above 49°N.

For 1981–2016, point observations provide the best available multi-decadal data for analyzing snowpack prediction skill. Available longer-term reanalysis products from data assimilation systems and precipitation station observations have been shown to have negative biases in precipitation accumulation in mountainous regions, making SWE point observations a useful independent measure of remote mountain precipitation (30, 45). As more products become available with longer records, they can be incorporated into prediction system initialization and verification like that from the Airborne Snow Observatory (46). We have used an additional reanalysis product from University of California, Los Angeles (36), available only over California from 1985 to the present, for additional verification. Further details can be found in *SI Appendix*.

Regional analysis uses mountain ranges defined similarly to ref. 47, with an additional criteria of mountain grid points in the AOGCMs having SWE in the 1981–2016 simulated climatology exceeding 2 cm (*SI Appendix, Fig. S1*). Unlike ref. 47, the Sierra Nevada has also been split into a northern and southern portion. For mountain range snowpack comparisons (Fig. 3 and *SI Appendix, Fig. S7*), snowpack was regridded to a common 50-km grid for prediction analysis and consistency with Fig. 4.

**Model Hindcasts.** The model hindcasts presented are dynamically produced by three GFDL AOGCMs: Coupled Model version 2.1, Forecast-Oriented Low Ocean Resolution (FLOR) Model, and HiFLOR (High-Resolution FLOR), referred to in the text as the 200-km, 50-km, and 25-km or low-, medium-, and high-resolution models, respectively, for simplicity (22, 27, 28). These models share common physics and ocean components, but differ in their horizontal resolution of the atmosphere and land surface to conservatively use computational resources for seasonal predictions. The lowest-resolution model (200 km) has a similar atmospheric/land resolution to the typical Coupled Model Intercomparison Project phase 5 (CMIP5) model. The medium-resolution atmospheric/land model configuration (50 km) has been shown to successfully reproduce the hydroclimate seasonal cycle over High Mountain Asia, where CMIP5 models fail to properly resolve complex topography (48). The highest-resolution configuration (25 km) was first developed for tropical cyclone research, producing category 4 and 5 storms, previously elusive at lower resolutions (28).

The 200- and 50-km models have provided operational seasonal predictions for the North American Multimodel Ensemble, an operational prediction system provided on a monthly basis for a limited number of variables (1981 to present at [www.cpc.ncep.noaa.gov/products/NMME](http://www.cpc.ncep.noaa.gov/products/NMME)) (13). This prediction system and July 1 start date has previously shown promise for seasonal prediction of tropical cyclones, with the highest-resolution model outperforming its counterparts (27, 28). Each ensemble member was made on July 1 for each year (1980–2015) and run for 12 mo to provide predictions of March snowpack (1981–2016, available at <http://data1.gfdl.noaa.gov>). We use the monthly mean SWE variable for each grid cell, which provides the water equivalent depth of the total column of snow on the land surface. Daily snowpack values are unavailable for the prediction experiments.

All models were initialized by using the same 12-member ensemble suite generated with the GFDL Ensemble Coupled Data Assimilation (ECDA) system (29) to produce 1,224 model years. Each ensemble member provides unique ocean assimilations from the ECDA to generate seasonal predictions with a coupled global climate model. The 200-km model is run with 10 ECDA ensemble members. The number of ensemble members for the higher-resolution models (50 km and 25 km) was increased to 12, given sensitivity testing for tropical cyclone prediction (28) and the assumption that higher-resolution models need more ensemble members due to greater internal variability (29). We did not increase the number of ensemble members for the 200-km model, out of a desire for computational efficiency, availability, and early analysis showing that 10 were sufficient (29). For the three models described here, the lowest-resolution 200-km model used ~750 computer processing unit (CPU) h per model year to run for its 10-member ensemble. Increasing the resolution to a 12-member ensemble at 50 and 25 km corresponds to a cost of 20,000 CPU h and 240,000 CPU h, respectively, per model year. To be clear, these are computational costs on a super computer and not real-time hours.

For the 50-km model, the ECDA ensemble members are divided into three subsets (1 through 4, 5 through 8, and 9 through 12) and are paired with three separately generated atmospheric/land initial conditions for each year from uncoupled (no dynamic ocean) atmosphere/land-only simulations for each model forced by sea surface temperatures (49) and historic radiative forcing values. For the 25-km model, the atmosphere/land components were initialized by three separate initial conditions (for ensemble members 1 through 4, 5 through 8, and 9 through 12) taken from an arbitrary year from the control

run simulation with fixed 1990 radiative forcing values, as an atmosphere-only simulation was not available. For the highest-resolution model, this means that the representative predictions come from the ocean state alone and may represent a lower bound on prediction skill. The assumption for this setup is that the atmospheric/land initial conditions provide fewer degrees of freedom in long multimonth seasonal predictions (8 mo here) than ocean initial conditions (42).

- Regonda S, Rajagopalan B, Clark M, Pitlick J (2005) Seasonal cycle shifts in hydroclimatology over the western United States. *J Clim* 18:372–384.
- Stewart I, Cayan D, Dettinger M (2005) Changes toward earlier streamflow timing across western North America. *J Clim* 18:1136–1155.
- Barnett TP, et al. (2008) Human-induced changes in the hydrology of the western United States. *Science* 319:1080–1083.
- Barnett TP, Adam JC, Lettenmaier DP (2005) Potential impacts of a warming climate on water availability in snow-dominated regions. *Nature* 438:303–309.
- Kapnick S, Hall A (2012) Causes of recent changes in western North American snowpack. *Clim Dyn* 38:1885–1899.
- Mote P, Hamlet A, Clark M, Lettenmaier D (2005) Declining mountain snowpack in western North America. *Bull Am Meteorol Soc* 86:39–46.
- Pederson GT, et al. (2011) The unusual nature of recent snowpack declines in the North American cordillera. *Science* 333:332–335.
- Sacramento Bee (June 6, 2015), Imperiled fish add to California's drought stress. Available at [www.sacbee.com/news/state/california/water-and-drought/article23294532.html](http://www.sacbee.com/news/state/california/water-and-drought/article23294532.html). Accessed May 23, 2016.
- McKelvey KS, et al. (2011) Climate change predicted to shift wolverine distributions, connectivity, and dispersal corridors. *Ecol Appl* 21:2882–2897.
- Westerling AL, Hidalgo HG, Cayan DR, Swetnam TW (2006) Warming and earlier spring increase western U.S. forest wildfire activity. *Science* 313:940–943.
- Cane MA, Zebiak SE, Dolan SC (1986) Experimental forecasts of El Niño. *Nature* 321:827–832.
- Jia L, DelSole T (2012) Multi-year predictability of temperature and precipitation in multiple climate models. *Geophys Res Lett* 39:L17705.
- Kirtman BP, et al. (2014) The North American multimodel ensemble: Phase-1 seasonal-to-interannual prediction; phase-2 toward developing intraseasonal prediction. *Bull Am Meteorol Soc* 95:585–601.
- McCabe GJ, Dettinger D (2002) Primary modes and predictability of year-to-year snowpack variations in the western United States from teleconnections with Pacific Ocean climate. *J Hydrometeorol* 3:13–25.
- Seager R, Kushnir Y, Nakamura J, Ting M, Naik N (2010) Northern Hemisphere winter snow anomalies: ENSO, NAO and the winter of 2009/10. *Geophys Res Lett* 37:L14703.
- Clark MP, Serreze MC, McCabe GJ (2001) Historical effects of El Niño and La Niña events on the seasonal evolution of the montane snowpack in the Columbia and Colorado River Basins. *Water Resour Res* 37:741–757.
- Cayan DR (1996) Interannual climate variability and snowpack in the western United States. *J Clim* 9:928–948.
- Mote PW (2006) Climate-driven variability and trends in mountain snowpack in western North America. *J Clim* 19:6209–6220.
- Abatzoglou JT (2011) Influence of the PNA on declining mountain snowpack in the western United States. *Int J Climatol* 31:1135–1142.
- Guan B, Waliser DE, Molotch NP, Fetzer EJ, Neiman PJ (2012) Does the Madden–Julian oscillation influence wintertime atmospheric rivers and snowpack in the Sierra Nevada? *Mon Weather Rev* 140:325–342.
- van der Wiel K, et al. (2016) The resolution dependence of contiguous U.S. precipitation extremes in response to CO<sub>2</sub> forcing. *J Clim* 29:7991–8012.
- Guan B, Molotch NP, Waliser DE, Fetzer EJ, Neiman PJ (2010) Extreme snowfall events linked to atmospheric rivers and surface air temperature via satellite measurements. *Geophys Res Lett* 37:L20401.
- Xiang B, et al. (2015) The 3–4-week MJO prediction skill in a GFDL coupled model. *J Clim* 28:5351–5364.
- Seo KH, et al. (2009) Evaluation of MJO forecast skill from several statistical and dynamical forecast models. *J Clim* 22:2372–2388.
- Jia L, et al. (2015) Improved seasonal prediction of temperature and precipitation over land in a high-resolution GFDL climate model. *J Clim* 28:2044–2062.
- Delworth TL, et al. (2006) GFDL's CM2 global coupled climate models. Part I: Formulation and simulation characteristics. *J Clim* 19:643–674.
- Vecchi GA, et al. (2014) On the seasonal forecasting of regional tropical cyclone activity. *J Clim* 27:7994–8016.
- Murakami H, et al. (2015) Simulation and prediction of category 4 and 5 hurricanes in the high-resolution GFDL HiFLOR coupled climate model. *J Clim* 28:9058–9079.
- Chang YS, Zhang S, Rosati A, Delworth TL, Stern WF (2013) An assessment of oceanic variability for 1960–2010 from the GFDL ensemble coupled data assimilation. *Clim Dyn* 40:775–803.
- Kapnick SB, Delworth TL (2013) Controls of global snow under a changed climate. *J Clim* 26:5537–5562.
- Feldstein SB (2000) The timescale, power spectra, and climate noise properties of teleconnection patterns. *J Clim* 13:4430–4440.
- Yang X, et al. (2015) Seasonal predictability of extratropical storm tracks in GFDL's high-resolution climate prediction model. *J Clim* 28:3592–3611.
- Lundquist JD, et al. (2015) High-elevation precipitation patterns: Using snow measurements to assess daily gridded datasets across the Sierra Nevada, California. *J Hydrometeorol* 16:1773–1792.
- Huning LS, Margulis SA (2017) Climatology of seasonal snowfall accumulation across the Sierra Nevada (USA): Accumulation rates, distributions, and variability. *Water Resour Res* 53:6033–6049.
- Klos PZ, Link TE, Abatzoglou JT (2014) Extent of the rain-snow transition zone in the western US under historic and projected climate. *Geophys Res Lett* 41:4560–4568.
- Margulis SA, Cortes G, Giroto M, Durand M (2016) A Landsat-era Sierra Nevada (USA) snow reanalysis (1985–2015). *J Hydrometeorol* 17:1203–1221.
- Smith DM, et al. (2007) Improved surface temperature prediction for the coming decade from a global climate model. *Science* 317:796–799.
- Dee DP, et al. (2011) The ERA-Interim reanalysis: Configuration and performance of the data assimilation system. *Q J R Meteorol Soc* 137:553–597.
- Diffenbaugh NS, Swain DL, Touma D (2015) Anthropogenic warming has increased drought risk in California. *Proc Natl Acad Sci USA* 112:3931–3936.
- Koster RD, Suarez MJ, Heiser M (2000) Variance and predictability of precipitation at seasonal-to-interannual timescales. *J Hydrometeorol* 1:26–46.
- Hughes M, Hall A, Fovell RG (2009) Blocking in areas of complex topography, and its influence on rainfall distribution. *J Atmos Sci* 66:508–518.
- Shukla S, Lettenmaier DP (2011) Seasonal hydrologic prediction in the United States: Understanding the role of initial hydrologic conditions and seasonal climate forecast skill. *Hydrol Earth Syst Sci* 15:3529–3538.
- Entin JK, et al. (2000) Temporal and spatial scales of observed soil moisture variations in the extratropics. *J Geophys Res Atmos* 105:11865–11877.
- Kapnick SB, Hall AD (2010) Observed climate–snowpack relationships in California and their implications for the future. *J Clim* 23:3446–3456.
- Henn B, et al. (2018) Spatiotemporal patterns of precipitation inferred from streamflow observations across the Sierra Nevada mountain range. *J Hydrol* 556:993–1012.
- Painter TH, et al. (2016) The Airborne Snow Observatory: Fusion of scanning lidar, imaging spectrometer, and physically-based modeling for mapping snow water equivalent and snow albedo. *Remote Sens Environ* 184:139–152.
- Pierce DW, Cayan DR (2013) The uneven response of different snow measures to human-induced climate warming. *J Clim* 26:4148–4167.
- Kapnick SB, Delworth TL, Ashfaq M, Malyshev S, Milly PCD (2014) Snowfall less sensitive to warming in Karakoram than in Himalayas due to a unique seasonal cycle. *Nat Geosci* 7:834–840.
- Reynolds RW, Rayner NA, Smith TM, Stokes DC, Wang W (2002) An improved in situ and satellite SST analysis for climate. *J Clim* 15:1609–1625.